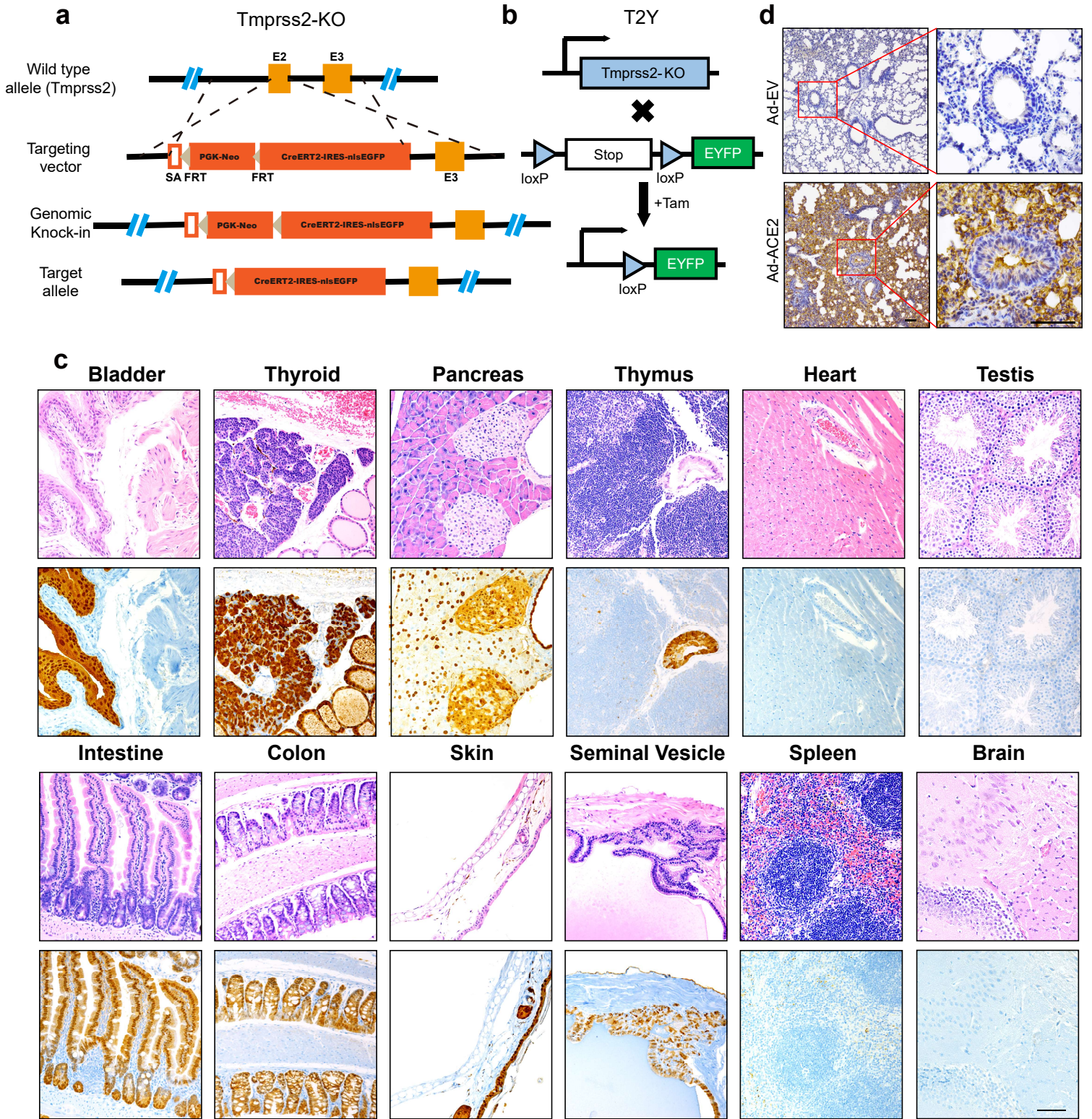
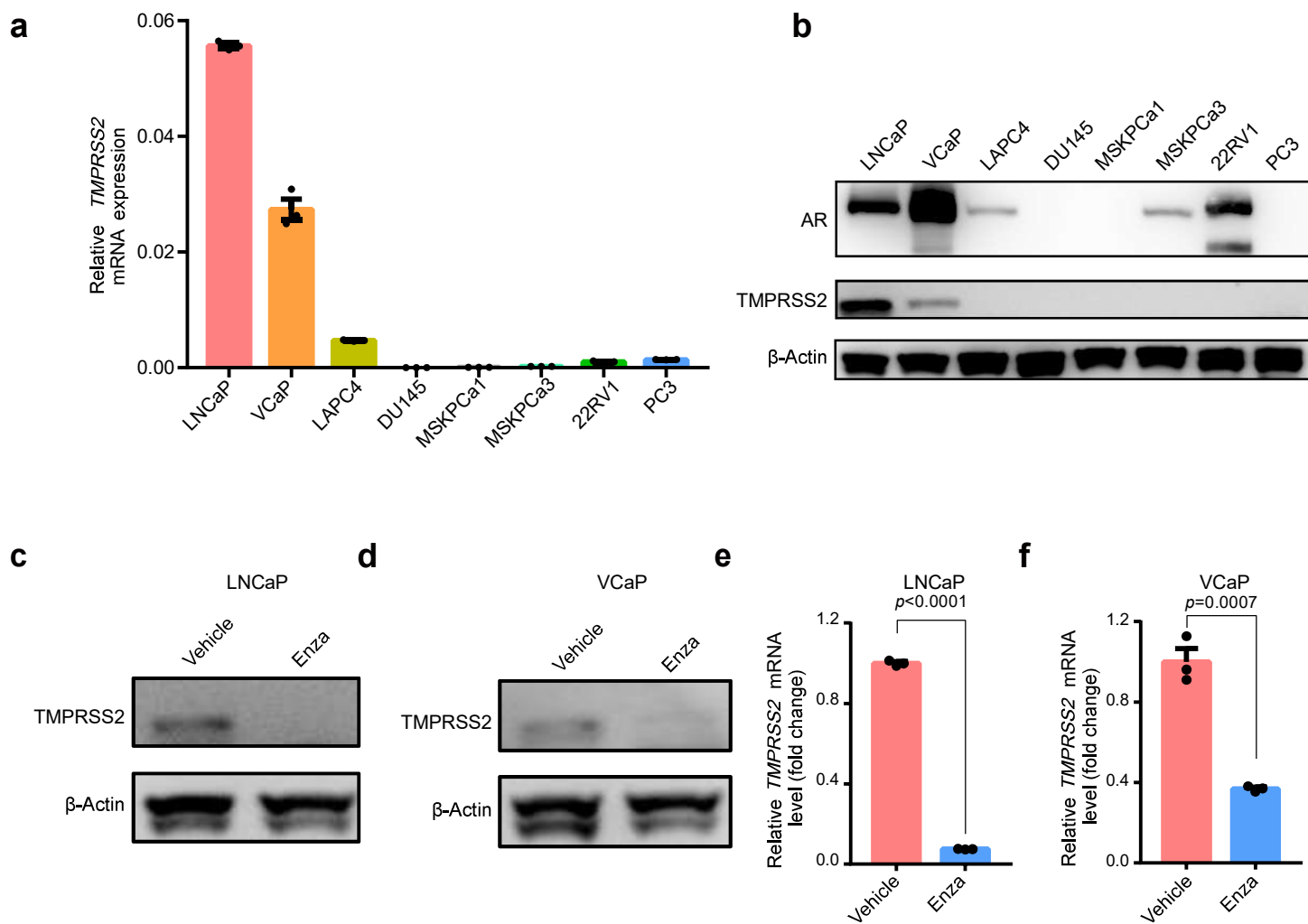


# Extended Data Figure 1



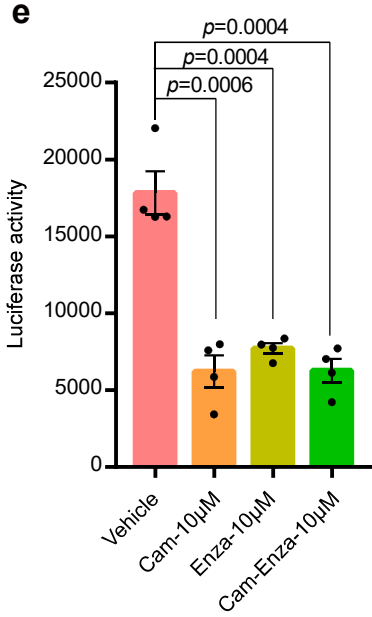
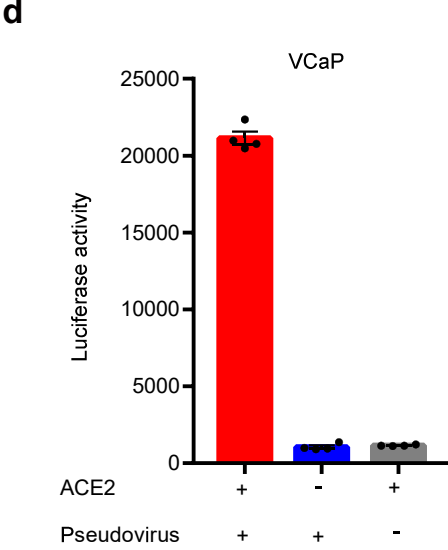
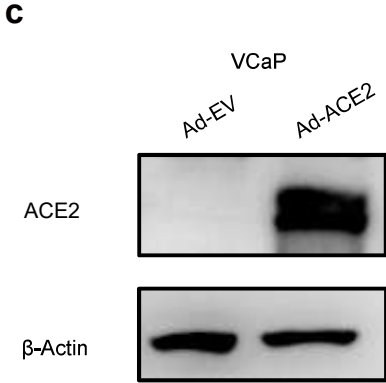
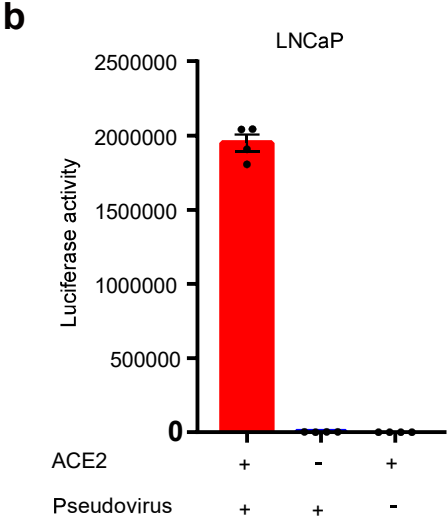
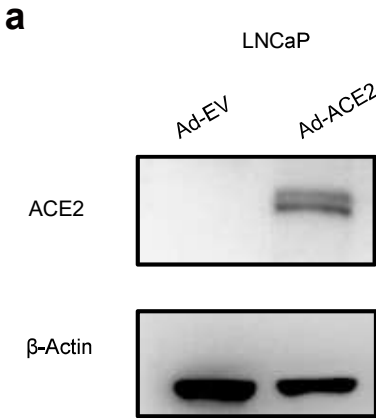
**Extended Data Figure 1 Identification of Tmprss2-positive cells in multiple mouse organs. (a)** Construction strategy for Tmprss2-KO mice. **(b)** Breeding strategy for the generation of T2Y mice. **(c)** YFP IHC staining for multiple organs of T2Y mice with tamoxifen gavage. **(d)** FLAG IHC staining in the lungs of WT transduced with Ad-EV (top) or Ad-ACE2 transduction (bottom), samples were collected 5 days post transduction.

## Extended Data Figure 2



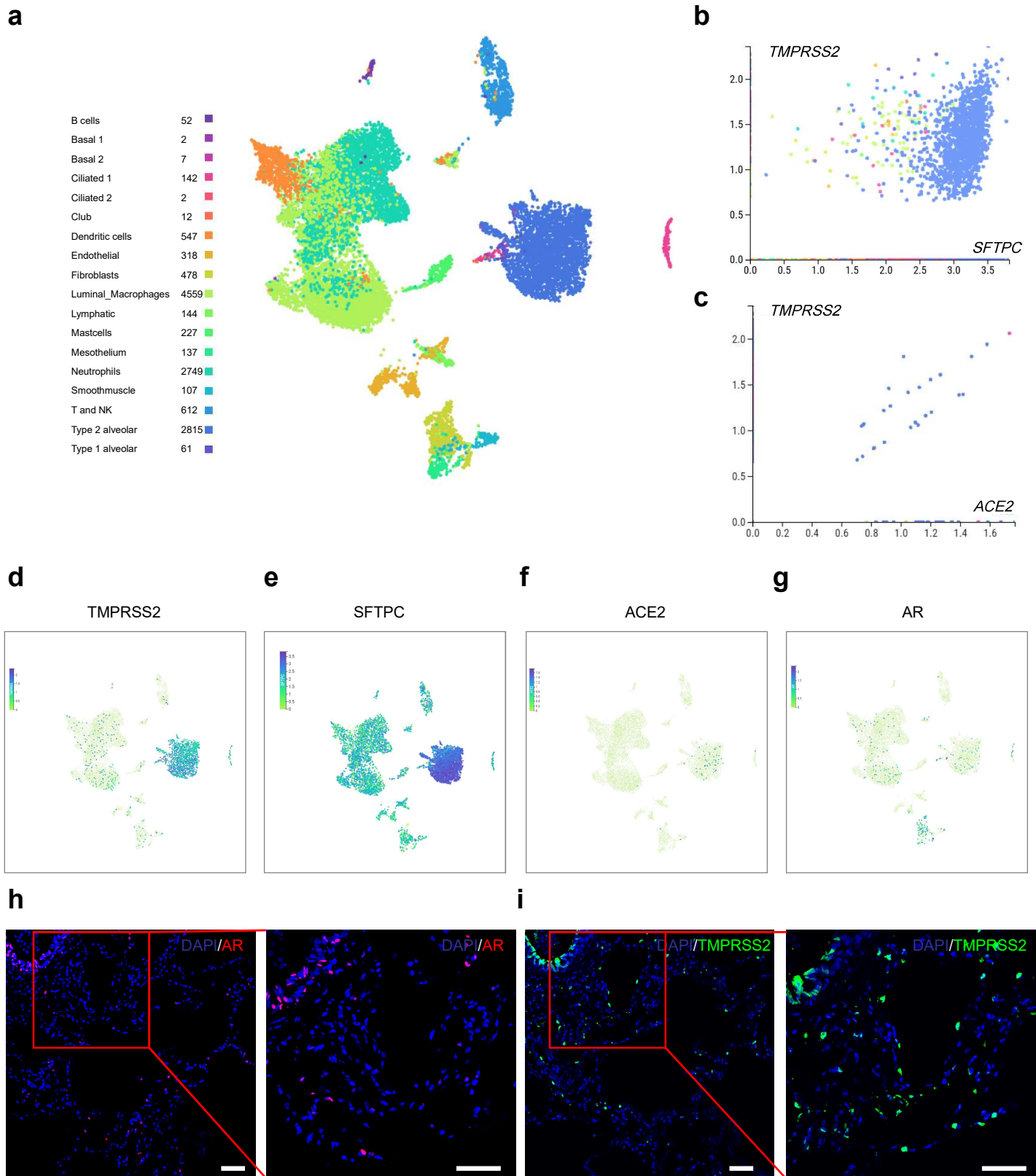
**Extended Data Figure 2 TMPRSS2 expression is reduced by enzalutamide in LNCaP and VCaP cells.** (a) qRT-PCR analysis of *TMPRSS2* mRNA expression in multiple prostate cancer cell lines and two prostate cancer organoid lines. (b) Western blotting analysis of TMPRSS2 and AR expression in multiple prostate cancer cell lines and two prostate cancer organoid lines. (c) Western blotting analysis of TMPRSS2 expression in LNCaP cells treated with vehicle under normal FBS condition or enzalutamide treatment under charcoal stripped FBS condition. (d) Western blotting analysis of TMPRSS2 expression in VCaP cells treated with vehicle under normal FBS condition or enzalutamide treatment under charcoal stripped FBS condition. (e) qRT-PCR analysis of *TMPRSS2* mRNA expression in LNCaP cells treated with vehicle under normal FBS condition or enzalutamide treatment under charcoal stripped FBS condition (two-tailed t-test, mean  $\pm$  SEM, n=3). (f) qRT-PCR analysis of *TMPRSS2* mRNA expression in VCaP cells treated with vehicle under normal FBS condition or enzalutamide treatment under charcoal stripped FBS condition (two-tailed t-test, mean  $\pm$  SEM, n=3).

# Extended Data Figure 3



**Extended Data Figure 3 Enzalutamide significantly reduces infection of VCaP cell with SARS-CoV-2-S.** (a) Western blotting analysis of ACE2 and  $\beta$ -Actin expression in LNCaP cells with empty vector adenovirus transduction or ACE2 adenovirus transduction. (b) SARS-CoV-2-S-driven entry into LNCaP cells with or without Ad-ACE2 transduction. Luciferase activity was measured 48 hours post SARS-CoV-2-S infection. (c) Western blotting analysis of ACE2 and  $\beta$ -Actin expression in VCaP cells with empty vector adenovirus transduction or ACE2 adenovirus transduction. (d) SARS-CoV-2-S-driven entry into VCaP cells with or without Ad-ACE2 transduction, luciferase activity was measured 48 hours post SARS-CoV-2-S infection. (e) SARS-CoV-2-S-driven entry into VCaP cells with Ad-ACE2 transduction treated with vehicle, 10  $\mu$ M camostat mesylate, 10  $\mu$ M enzalutamide and 10  $\mu$ M camostat mesylate/enzalutamide. Luciferase activity was measured 48 hours post SARS-CoV-2-S infection (two-tailed t-test, mean  $\pm$  SEM, n=4).

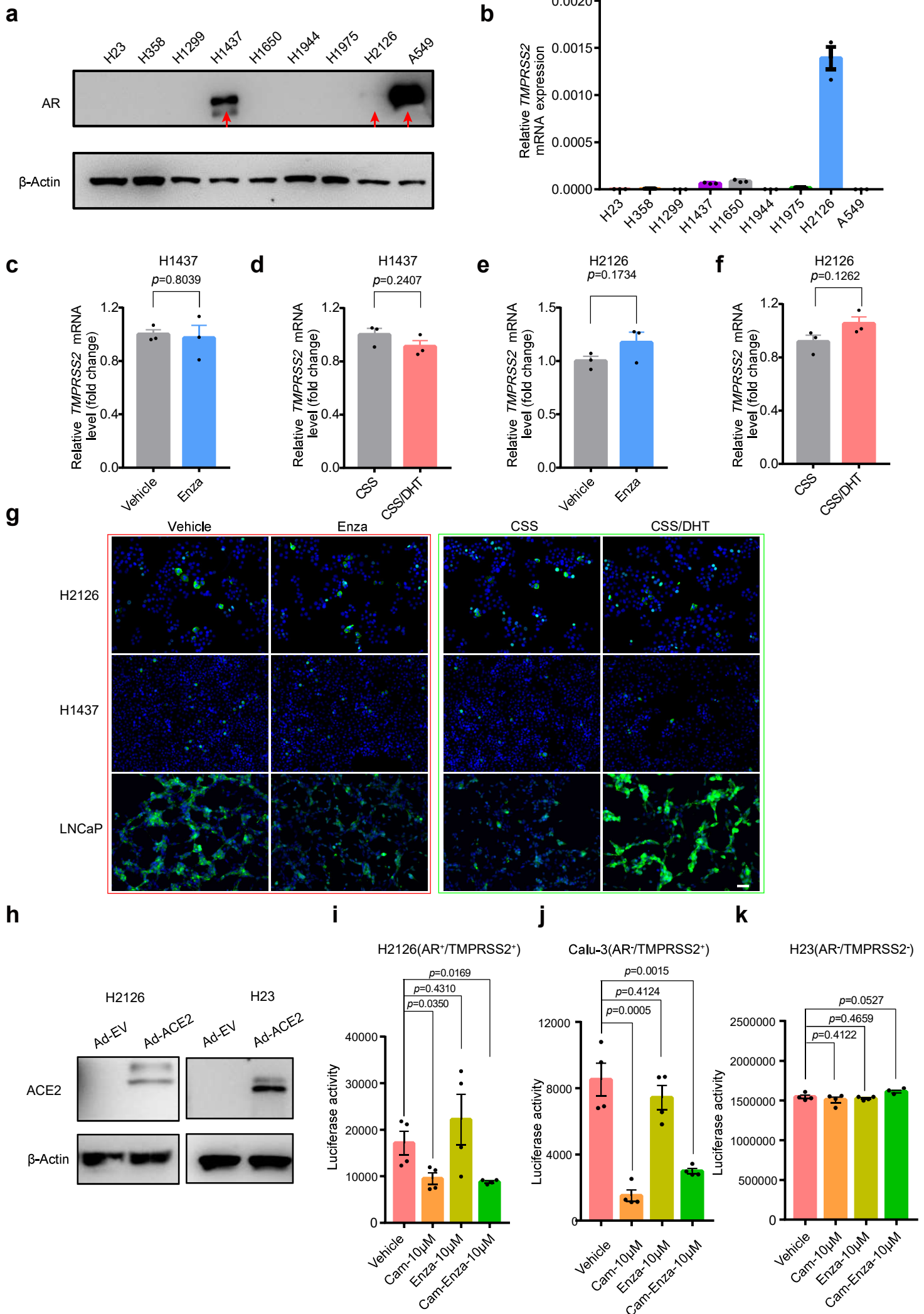
# Extended Data Figure 4



**Extended Data Figure 4 AR-positive and TMPRSS2-positive cells are verified in human lungs. (a)** UMAP plot displaying cell clusters of human airway epithelial cells from a public dataset using COVID-19 Cell Atlas. **(b)** *TMPRSS2* and *SFTPC* mRNA expression across multiple cell types. **(c)** *TMPRSS2* and *ACE2* mRNA expression across multiple cell types. **(d-g)** *TMPRSS2* **(d)**, *SFTPC* **(e)**, *ACE2* **(f)** and *AR* **(g)** mRNA expression levels on UMAP plots across multiple cell types. **(h-i)** Immunofluorescence staining of AR **(h)** and *TMPRSS2* **(i)** in human lungs using adjacent sections. Scale bars represent 50  $\mu\text{m}$ .



# Extended Data Figure 5

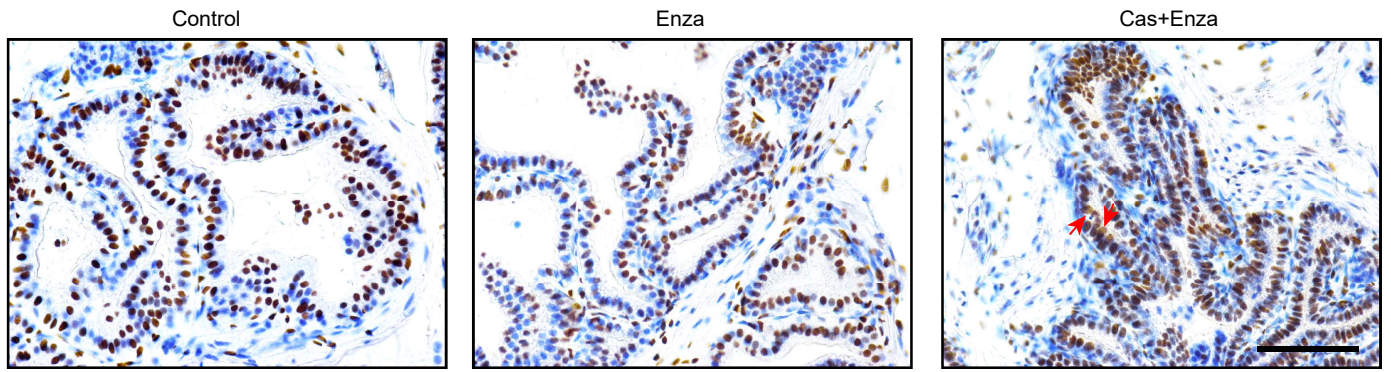


**Extended Data Figure 5 Enzalutamide does not prevent SARS-CoV-2-S-driven entry into lung cells.**

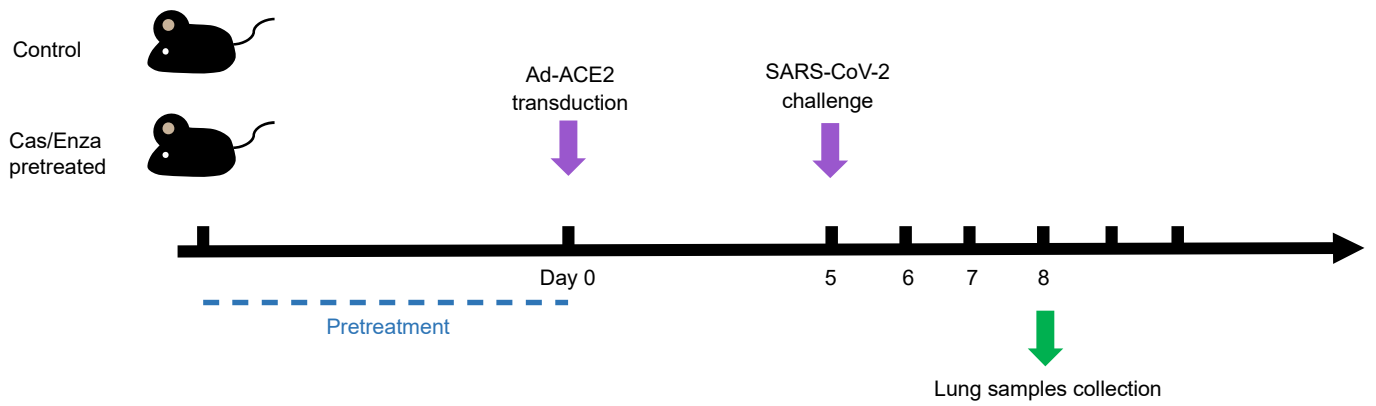
**(a)** Western blotting analysis of AR expression in multiple lung cancer cells. **(b)** qRT-PCR analysis of *TMPRSS2* mRNA expression in multiple lung cancer cells. **(c)** qRT-PCR analysis of *TMPRSS2* mRNA expression in H1437 cells with vehicle or enzalutamide treatment. **(d)** qRT-PCR analysis of *TMPRSS2* mRNA expression in H1437 cells with or without DHT treatment under charcoal stripped FBS condition. **(e)** qRT-PCR analysis of *TMPRSS2* mRNA expression in H2126 cells with vehicle or enzalutamide treatment. **(f)** qRT-PCR analysis of *TMPRSS2* mRNA expression in H2126 cells with or without DHT treatment under charcoal stripped FBS condition. **(g)** Immunofluorescence staining of *TMPRSS2* in H2126 (top), H1437 (middle) and LNCaP (bottom) cells under multiple treatments condition. **(h)** Western blotting analysis of ACE2 and  $\beta$ -Actin expression in H2126 (left) and H23 (right) cells with empty vector adenovirus transduction or ACE2 adenovirus transduction respectively. **(i-k)** SARS-CoV-2-S-driven entry into H2126 **(i)**, Calu-3 **(j)** and H23 **(k)** cells transduced with Ad-ACE2 and treated with vehicle, 10  $\mu$ M camostat mesylate, 10  $\mu$ M enzalutamide and 10  $\mu$ M camostat mesylate/enzalutamide. Luciferase activity was measured 48 hours post SARS-CoV-2-S infection (two-tailed t-test, mean  $\pm$  SEM, n=4). Scale bars represent 50  $\mu$ m.

# Extended Data Figure 6

**a**

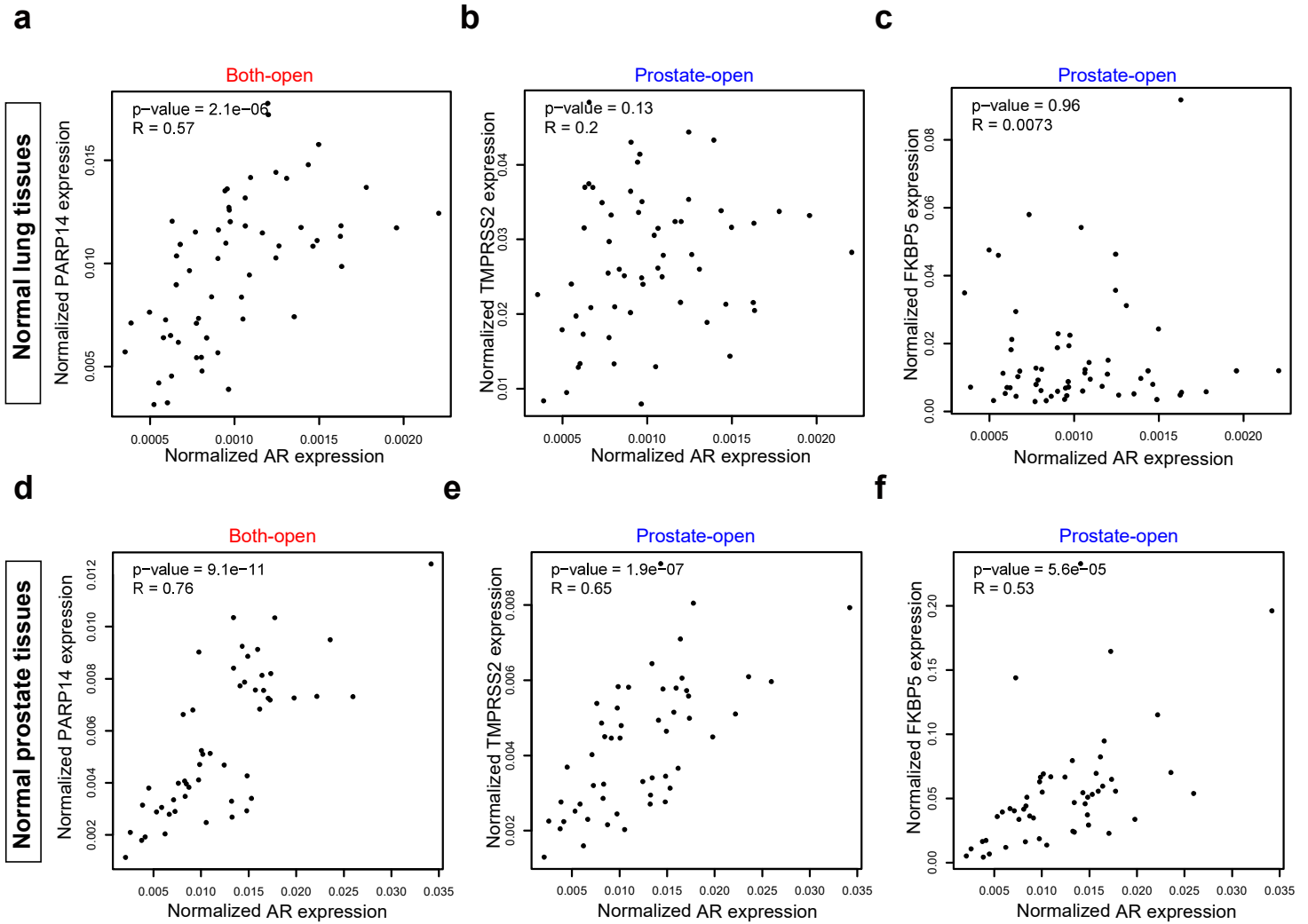


**b**



**Extended Data Figure 6 Ad-ACE2-transduced mouse models are employed to assess the efficacy of enzalutamide *in vivo*.** (a) IHC staining for AR in prostates of wild type mice, enzalutamide-treated mice and enzalutamide-treated castrated mice respectively. Red arrows indicate blocking of nuclear translocation of AR in prostates of enzalutamide treated castrated mice. (b) Schematic strategy for Ad-ACE2-transduced mouse to evaluate the therapeutic efficacy of enzalutamide.

# Extended Data Figure 7



**Extended Data Figure 7 Correlation analysis of mRNA levels of AR and TMPRSS2 in human lung tissues and prostate tissues. (a-c)** Correlation analysis for normalized expression of AR and a both-open gene *PARP14* (left) **(a)**, two prostate-open genes *TMPRSS2* (middle) **(b)** and *FKBP5* (right) respectively in normal lung tissues using TCGA datasets **(c)**. **(d-f)** Correlation analysis for normalized expression of *AR* and a both-open gene *PARP14* (left) **(d)**, two prostate-open genes *TMPRSS2* (middle) **(e)** and *FKBP5* (right) respectively in normal prostate tissues using TCGA datasets **(f)**.